Controlled Extracellular Matrix Degradation in Breast Cancer Tumors Improves Therapy by Trastuzumab

Ines Beyer[1], Zongyi Li[1], Jonas Persson[1], Ying Liu[1], Ruan van Rensburg[1], Roma Yumul[1], Xiao-Bing Zhang[2], Mien-Chie Hung[3] and André Lieber[1,4]

[1]Department of Medicine, Division of Medical Genetics, University of Washington, Seattle, Washington, USA; [2]Department of Medicine, University Division of Regenerative Medicine, Loma Linda University, Loma Linda, California, USA; [3]Department of Molecular and Cellular Oncology, University of Texas MD Anderson Cancer Center, Houston, Texas, USA; [4]Department of Pathology, University of Washington, Seattle, Washington, USA

Extracellular matrix (ECM) in solid tumors affects the effectiveness of therapeutics through blocking of intratumoral diffusion and/or physical masking of target receptors on malignant cells. In immunohistochemical studies of tumor sections from breast cancer patients and xenografts, we observed colocalization of ECM proteins and Her2/*neu*, a tumor-associated antigen that is the target for the widely used monoclonal antibody trastuzumab (Herceptin). We tested whether intratumoral expression of the peptide hormone relaxin (Rlx) would result in ECM degradation and the improvement of trastuzumab therapy. As viral gene delivery into epithelial tumors with extensive tumor ECM is inefficient, we used a hematopoietic stem cell (HSC)-based approach to deliver the *Rlx* gene to the tumor. In mouse models with syngeneic breast cancer tumors, HSC-mediated intratumoral Rlx expression resulted in a decrease of ECM proteins and enabled control of tumor growth. Moreover, in a model with Her2/*neu*-positive BT474-M1 tumors and more treatment-refractory tumors derived from HCC1954 cells, we observed a significant delay of tumor growth when trastuzumab therapy was combined with Rlx expression. Our results have implications for antibody therapy of cancer as well as for other anticancer treatment approaches that are based on T-cells or encapsulated chemotherapy drugs.

Received 24 August 2010; accepted 23 October 2010; published online 16 November 2010. doi:10.1038/mt.2010.256

INTRODUCTION

For the growth of solid tumors, the development of tumor stroma is essential. Tumor stroma is composed of stromal cells and a complexly structured extracellular matrix (ECM), containing collagen, laminin, hyaluronic acid, glycosaminoglycans, and proteoglycans. Stromal cells include fibroblasts, endothelial cells, pericytes, as well as tumor-infiltrating hematopoietic cells that are predominantly derived from myeloid-lineage progenitor cells located in the bone marrow. ECM components form extensive networks and connect to tumor cells via cellular integrins. ECM proteins are considered to be largely produced by tumor stroma cells. A recent study, however, indicated that tumor cells with mesenchymal features also express laminin, fibronectin, and collagen IV.[1] A series of reports demonstrated that ECM not only attenuates the efficacy of endogenous antitumor immune response, but also represents a barrier to therapeutic modalities, including antibodies,[2] immunotoxins,[3] T-cells,[4] interferons,[5] encapsulated chemotherapy drugs,[6] or oncolytic adenoviruses (Ads).[7] These studies show that the detrimental effect of tumor ECM on therapeutics is exerted through blocking of intratumoral diffusion and/or physical masking of target receptors on malignant cells. Attempts to overcome these problems include the application of ECM degrading enzymes. In preclinical models, it has been shown that collagenase increases the diffusion rate of immunoglobulin (Ig) G in tumors.[8,9] Injection of collagenase was also found to increase the uptake of therapeutic agents, for example liposomal doxorubicin (Caelyx) and antibodies against the osteosarcoma-associated antigen TP-2 in human osteosarcoma xenografts.[10,11] Furthermore, the direct administration of collagenase/dispase or trypsin into glioma xenografts enhanced the extent of infection of a nonreplicating Ad vector expressing a reporter gene.[12]

A protein that has been often used to degrade tumor ECM proteins is relaxin (Rlx), a peptide hormone that during pregnancy is involved in softening the uterine cervix, vagina, and interpubic ligaments in preparation for parturition.[13] This effect is achieved by decreasing the synthesis and secretion of interstitial collagens as well as the upregulating matrix metalloproteinase and collagenase expression.

Rlx has been tested as a therapeutic in preclinical models. In a mouse tumor model, the chronic application of Rlx via osmotic pumps resulted in collagen degradation and an increased intratumoral diffusion of macromolecules.[14] In cancer virotherapy studies, Ad-mediated Rlx expression enhanced the spread of oncolytic Ads in which transduction of non-Rlx-expressing virus was low overall.[15,16]

As noted above, the tumor ECM can affect the efficacy of transduction by Ads, including Ads that express Rlx. Furthermore, systemic application of viral vectors is hampered by immune responses and unspecific sequestration by nontumor tissues. We therefore

Correspondence: *André Lieber, Division of Medical Genetics, University of Washington, Box 357720, Seattle, Washington 98195, USA. E-mail: lieber00@u.washington.edu*

developed a new approach for gene delivery to tumors that is based on hematopoietic stem cells (HSCs). The approach capitalizes on the fact that most solid cancers are heavily infiltrated by tumor-associated macrophages (TAMs), whose progenitors are actively recruited by the tumor from bone-localized HSCs. Our approach involves the *ex vivo* transduction of HSCs with integrating viral vectors containing therapeutic transgenes and the transplantation of these cells into myelo-conditioned recipients, where they engraft in the bone marrow and provide a long-term source of genetically modified cells that will home to tumors. In a recent study, we showed that the inducible intratumoral expression of Rlx after the transplantation of mouse HSCs transduced with a Rlx-expressing lentivirus vector, delayed tumor growth in an immunocompetent mouse breast cancer model.[17] The antitumor effect of Rlx was mediated by the degradation of the tumor ECM proteins, which in turn provided pre-existing immune cells with increased access to the tumor. Here, we will use this HSC-based gene delivery approach in xenograft models of breast cancer in combination with anti-Her2/*neu* antibody therapy.

Human epithelial growth factor receptor-2 (HER-2/*neu*) is a tumor antigen utilized as a prognosis factor as well as a vaccine/therapy target in breast cancer. Approximately 20–30% of all breast cancers are Her2/*neu* positive. This is combined with a poor prognosis for the patients.[18] The development of the monoclonal antibody trastuzumab (Herceptin) brought a significant improvement in the outcome of these patients. Trastuzumab has become part of first line therapy for Her2/*neu*-positive breast cancer patients. Unfortunately, a significant number of Her2/*neu*-positive patients do not respond to treatment with trastuzumab-containing regimens.[18] In this study, we observed extensive ECM and intercellular junctions in breast cancer patients and xenograft models. We hypothesized that this blocks the access to Her2/*neu* and/or the intratumoral dissemination of trastuzumab. Here, we show that a stem-cell based approach for Rlx expression in tumors mediates tumor ECM degradation and significantly improves trastuzumab therapy in two xenograft models.

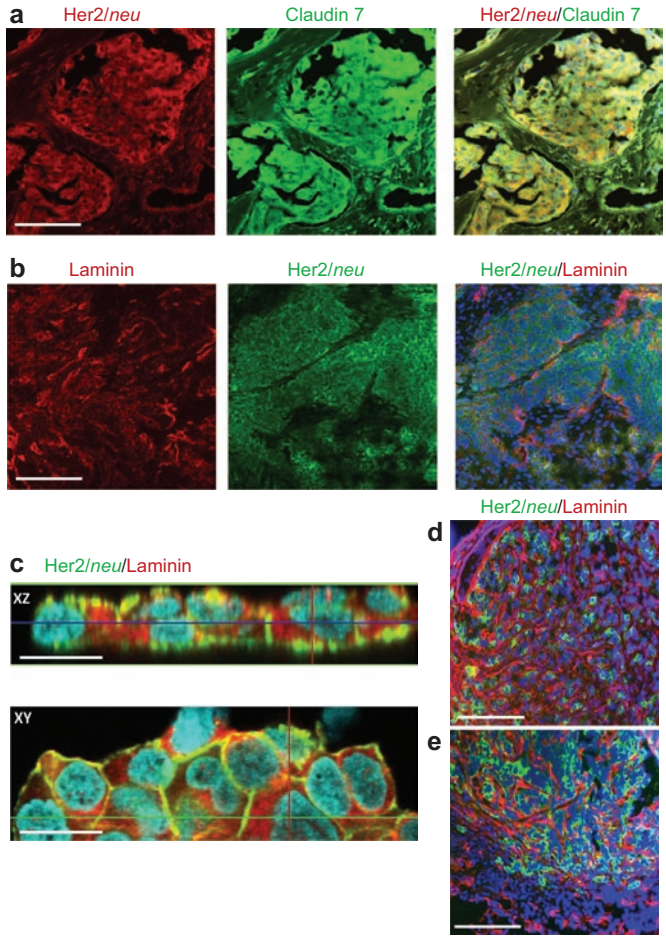

Figure 1 Immunohistochemical colocalization of Her2/*neu* and ECM proteins in breast cancer. (**a**) Representative sections of a tumor biopsy from a patient with stage III ductal mammary carcinoma. (**b**) Sections of a biopsy from a patient with stage IV clear cell ovarian cancer. Bar = 40 µm. (**c**) Confocal microscopy of BT474-M1 tumor cells *in vitro*. Shown are representative images of stacked XZ and XY sections. Bar = 20 µm. (**d**,**e**) Sections of xenograft tumors derived from (**d**) BT474-M1 and (**e**) HCC1954 cells. Bar = 40 µm. ECM, extracellular matrix.

RESULTS

Immunohistochemical colocalization of Her2/neu and ECM proteins

As outlined above, tumor ECM affects the transport of antibodies from the blood vessels to tumor cells and intratumoral dissemination. We also hypothesized that ECM proteins mask target receptors on the tumor cell surface and affect access of therapeutic antibodies such as trastuzumab. This is supported by immunohistochemical studies of Her2/*neu* and tight junction protein Claudin 7 and the ECM protein laminin on Her2/*neu*-positive breast and ovarian cancer biopsies (**Figure 1a,b**, respectively). Overlapping signals for Her2/*neu* and ECM protein were observed in focal microscopy studies on established breast cancer cell lines, *e.g.*, BT474-M1 (**Figure 1c**). Furthermore, when transplanted into the mammary fat pad of immunodeficient CB17 SCID-beige, the Her2/*neu*-positive human breast cancer cell lines BT474-M1 and HCC1954 formed tumor nests surrounded by tumor ECM costaining of Her2/*neu* and laminin (**Figure 1d,e**). Therefore, both tumor models adequately reflect key features of human breast cancer tumors *in situ*, *i.e.*, widespread tumor stroma and masking of Her2/*neu* by ECM proteins.

Lentivirus vectors for regulated Rlx expression

Our stem cell gene therapy approach is based on the transduction of HSCs with integrating gene transfer vectors and subsequent doxycycline (Dox)-regulated transgene expression from HSC-derived TAMs. Previously, using a lentivirus vector for Dox-inducible transgene expression, we found high background Rlx expression in cells and animals without Dox induction.[19] As retroviruses integrate preferentially into genes, this could be the result of unspecific activation of transgene expression by chromosomal transcription elements and/or the interference between the retroviral promoters/enhancers within the proviral long-terminal repeat with the Dox-inducible expression cassette. To address these problems we constructed self-inactivating (SIN) lentivirus vectors, *i.e.*, vectors containing a deletion within the 3′ long-terminal repeat, which abolishes the long-terminal repeat promoter activity (**Figure 2a**). In addition to the U3 deletion, the long-terminal

a

b

Clones	Powered ΔCt (w/ Dox)	Powered ΔCt (w/o Dox)	Fold induction of Rlx expression
1	8.2	17.0	441.4
2	4.2	16.5	5113.2
3	7.9	15.8	231.7
4	6.4	15.9	714.7
6	11.6	16.5	31.1
7	0.8	13.9	8841.0
8	4.8	19.9	8945.8
9	9.5	15.8	75.4
10	6.8	16.8	1077.1
11	8.4	15.5	550.3
12	2.0	16.9	40848.1
13	2.3	17.7	31254.3
14	9.7	16.1	85.2
15	9.5	16.3	115.2
16	11.8	16.7	30.4
17	7.3	13.5	74.6
18	9.7	17.9	291.8

Figure 2 Insulated SIN-lentivirus vector for regulated Rlx expression (Ins-SIN-LV-Rlx). (**a**) Scheme of integrated provirus. The *Rlx* gene is under the control of a tTR-KRAB system.[51] tRT-KRAB bound to tet-operator sequences represses promoters in the vicinity of 3–4 kb. Addition of Dox releases this repression. The vector also contains a central polypurine tract (cPPT) and a woodchuck hepatitis virus post-transcriptional regulatory element (WPRC). A 0.4-kb cHS4 insulator element[52] is inserted into the 398-bp U3 promoter/enhancer deletion (U3Δ). Upon proviral integration into host genome, the U3 region containing the cHS4 is copied over to the 5′ LTR. (**b**) BT474-M1 cells were transduced with VSV-G-pseudotyped Ins-SIN-LV-Rlx at an MOI of 1. Twenty-four hours after transduction, cells were subjected to limited dilution in 96-well plates. Individual colonies were expanded and treated with Dox for 24 hours. Then, mRNA was isolated and subjected to qRT-PCR for GAPDH and Rlx mRNA. The powered ΔCt values represent Rlx mRNA levels compared to GAPDH mRNA levels. The right column shows the induction factor upon Dox addition. Dox, doxycycline; LTR, long-terminal repeat; MOI, multiplicity of infection; qRT-PCR, quantitative reverse transcription; Rlx, relaxin; SIN, self-inactivating.

repeats also contained a chromatin insulator derived from the chicken globin locus control region DNase I hypersensitivity 4 region (cHS4). In the integrated provirus the transgene cassette is therefore flanked by two cHS4 insulators (**Figure 2a**). It has been shown that the cHS4 insulator protects retrovirus vectors from chromosomal position effects of integration and from silencing, particularly in HSCs and their progeny.[20,21] Notably, the vector contained the transgene under the control of the mouse phosphoglycerate kinase 1 promoter that is active in HSCs, their progeny, as well as in tumor cells. The Rlx expression cassette can be activated by the addition of Dox.

We tested a new insulated SIN lentivirus vector containing a Dox-inducible Rlx expression cassette (Ins-SIN-LV-Rlx) in a series of breast cancer cell lines. To assess potential chromosomal position effects, subsequent to transduction of cells with Ins-SIN-LV-Rlx at an multiplicity of infection of 1, individual clones were analyzed for Rlx mRNA levels by quantitative reverse transcription-PCR with and without Dox induction. Exemplary for these studies, **Figure 2b** shows data for BT474-M1-Rlx clones. The addition of Dox increased mRNA levels, on average, 5,509-fold in clones derived from Ins-SIN-LV-Rlx transduced cells. We also measured the ability of Rlx to stimulate cAMP production in cells.[22] In BT474-M1-Rlx clone #4, the clone that we used in subsequent *in vivo* studies, cAMP activity was 16-fold higher in culture supernatants 48 hours after the addition of Dox when compared to pretreatment levels. This indicates that Rlx expressed from Ins-SIN-LV-Rlx is catalytically active and that its production can be induced by Dox.

Effect of Rlx expression on trastuzumab killing *in vitro*

Our immunohistochemical studies indicated that ECM proteins mask Her2/*neu* in breast cancer cultures, implying that Rlx-mediated ECM protein degradation might increase killing by trastuzumab. We therefore utilized BT474-M1 clones transduced with Ins-SIN-LV-Rlx (BT474-M1-Rlx) with and without Dox treatment to test this hypothesis. Immunohistochemical studies of BT474-M1-Rlx demonstrated the presence of laminin in paracellular spaces with costaining of Her2/*neu*, and a decrease in laminin in the Dox-treated group (**Figure 3a**). To analyze access of therapeutics to Her2/*neu*, we measured cell viability of BT474-M1-Rlx cells after treatment with trastuzumab in the presence and absence of Dox (**Figure 3b**). In agreement with earlier studies,[23] incubation of Her2/*neu*-positive breast cancer cells with trastuzumab caused death of ~20% of cells. Induction of Rlx expression in BT474-M1-Rlx by Dox for 2 days, significantly increased trastuzumab killing. Trastuzumab or trastuzumab with Dox had no cytotoxic effect on the Her2/*neu*-negative breast cancer cell line MDA-MB-231-Rlx, which express Rlx at comparable levels to BT474-M1-Rlx (**Figure 3b**, lower panel). These *in vitro* findings create a basis for testing whether Rlx-mediated degradation of tumor stroma proteins can increase the therapeutic efficacy of trastuzumab *in vivo*.

Homing of gene modified bone marrow cells to MMC tumors

Our stem cell-based approach for gene delivery of Rlx to tumors is based on the active recruitment of bone-marrow localized TAM progenitors by the tumor. The approach involves the *ex vivo* transduction of HSCs with lentiviral vectors. As it was unclear prior to this study whether human xenograft tumors could mobilize and attract mouse TAM progenitors, we first tested our new Ins-SIN-LV-Rlx vector in a syngeneic system involving transduction of mouse bone marrow HSCs. We used FVB/N-TgN 220-MMTV/*neu* mice that overexpress rat *neu* in breast tissue (*neu*-tg mice). Mouse mammary carcinoma cells (MMC) is a transplantable carcinoma line derived from a spontaneous mammary tumor from *neu*-tg mice.[24] Our previous studies have shown that MMC cells form tumor nests surrounded by laminin. Tumor stroma is infiltrated with leukocytes. Leukocytes are separated from MMC cells by tumor stroma proteins. Despite the presence of tumor-specific, $CD8^+$ cells in MMC tumors, tumor progression cannot be controlled, which appears, in part, to be due to physical barriers.[19]

As a source of HSCs, we used bone marrow cells from mice that were injected intravenously with 5-fluorouracil (150 mg/kg) 2 days before the collection of the bone marrow. Bone marrow cells were cultured for 3 days and nonadherent cells (enriched for HSCs and primitive progenitors) were mock-transduced or tranduced with a green fluorescent protein (GFP)-expressing LV vector at a multiplicity of infection of 2. Transduced cells were then transplanted into lethally irradiated *neu*-tg mice. Six weeks

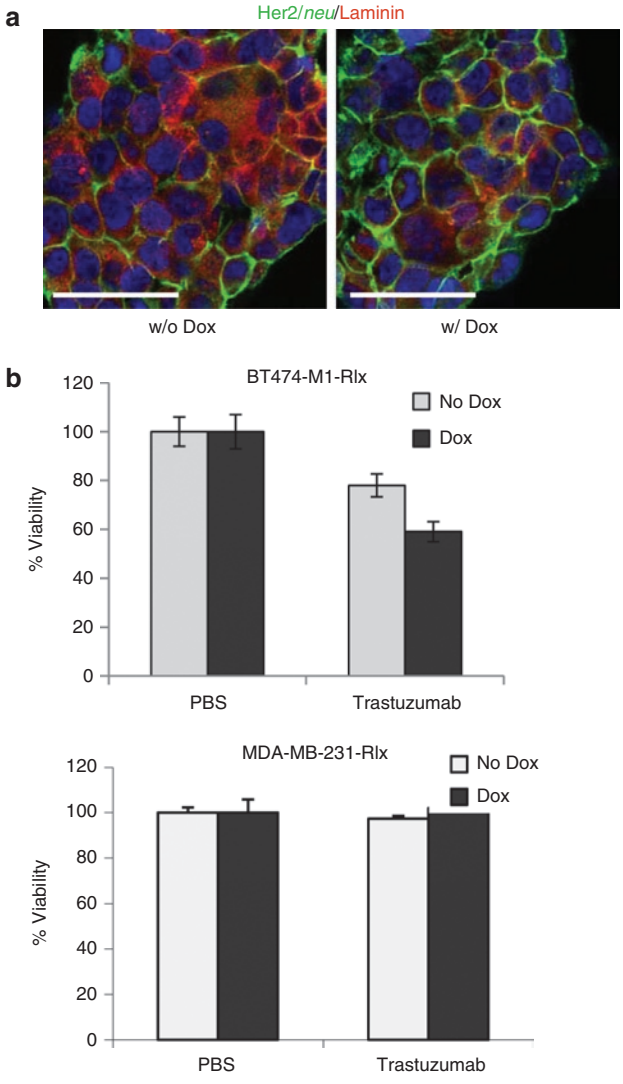

Figure 3 Effect of Dox-induced Rlx expression on trastuzumab killing *in vitro*. These studies used BT474-M1-Rlx clone #4 (see **Figure 2b**) and a MDA-MB-231-Rlx clone with a comparable Rlx mRNA expression level. (**a**) Immunofluorescent analysis of BT474-M1-Rlx clone #4 for laminin and Her2/*neu* 2 days after Dox addition. (**b**) *In vitro* killing of (Her2/*neu*-positive) BT474-M1-Rlx and (Her2/*neu*-negative) MDA-MB-231-Rlx cells by trastuzumab. BT474-M1-Rlx cells were grown to confluence, incubated with Dox (1 µg/ml) or PBS for 2 days and then treated with trastuzumab (15 µg/ml) for 30 minutes. Cell viability was measured 2 hours later by WST-1 assay. Viability of PBS-treated cells was taken as 100%. $N = 5$, $^*P < 0.05$ for BT474-M1-Rlx+trastuzumab w/ Dox versus w/o Dox. Three independent experiments were performed and the data used for statistical analysis. Dox, doxycycline; PBS, phosphate-buffered saline; Rlx, relaxin.

later, subsequent to the bone marrow engraftment of genetically modified cells, mice were subcutaneously injected with MMC cells. Dox was intraperitoneally injected at day 7 and then every other day (**Figure 4a**). When analyzed before transplantation 47(+/−11)% of HSC cells expressed GFP after *ex vivo* LV transduction (**Figure 4b**, left panel). In MMC tumors, we found large numbers of GFP-marked transplanted donor cells localized to the tumor stroma (**Figure 4b**, right panel). Flow cytometry analyses of a cell suspension of explanted MMC tumors showed that a total of 4.65 (+/−1.1)% of all tumor cells (including stroma and malignant cells) were GFP$^+$ and that approximately half of the GFP$^+$ cells were also positive for the macrophage marker F4/80 (**Figure 4b**, left panel). This study shows efficient transgene delivery to the center of tumors using *ex vivo* transduced HSCs as a vehicle.

To validate the function of Ins-SIN-LV-Rlx in the MMC/*neu*-tg mouse model, HSC were transduced with this vector and transplanted as described above. Seven days after MMC cell transplantation, Rlx was induced by intraperitoneal Dox injection and tumor growth monitored. Mice that received Ins-SIN-LV-Rlx transduced HSCs and Dox treatment had significantly smaller tumors compared to animals without Dox induction and to animals that received mock-transduced bone marrow cells (**Figure 4c**). Sections from tumors harvested at day 19 after MMC cell transplantation were stained for the basement membrane using Jones' methenamine silver staining method[25] (**Figure 4d**). Less and more fragmented basement membrane fibers were found in animals that expressed Rlx. We also performed immunohistochemistry for the ECM protein collagen IV and quantified signals by morphometry. The area of collagen IV per section was 11.5(+/−1.3)% for Tx(Mock), 13.3+/−1.8% for Tx(Mock)+Dox, 7.5(+/−0.8%) for Tx(Rlx), and 6.7+/−0.8% for Tx(Rlx)+Dox [$P < 0.05$ for Tx(Mock) versus Tx(Rlx) and Tx(Mock)+Dox versus Tx(Rlx)+Dox]. This indicates that the Rlx-mediated decrease in tumor collagen IV enables control of tumor growth. Notably, no side effects (weight loss, hematological abnormalities, abnormal organ histology) were observed in mice with Dox-induced Rlx expression, indicating that Rlx expression from HSCs and their progeny at extratumoral sites did not cause critical toxicity.

Infiltration of breast cancer xenograft tumors by mouse TAMs

Rat Her2/*neu* (in *neu*-tg mice) does not react with trastuzumab. We therefore tested the effect of Rlx-mediated tumor ECM protein degradation on trastuzumab therapy in xenograft models with tumors derived from the Her2/*neu*-positive human breast cancer cell lines BT474-M1 and HCC1954. Analysis of tumor sections derived from BT474-M1 cells (**Figure 5a**) or HCC1954 cells (**Figure 5b**) showed efficient vascularization and infiltration with mouse CD45$^+$ and F4/80$^+$ TAMs that were predominantly localized to the tumor stroma. This histology implies that mouse bone marrow-derived HSCs can be used to deliver a transgene to the xenograft tumor.

Effect of Rlx on trastuzumab therapy *in vivo*

Using the stem cell-based gene delivery approach in BT474-M1 and HCC195 xenograft tumor models, we tested whether (i) Dox-induced Rlx expression had therapeutic effects and (ii) whether Rlx-induced ECM degradation improved trastuzumab therapy.

We first performed *in vivo* studies in the BT474-M1 model. We transduced mouse bone marrow cells with Ins-SIN-LV-Rlx and transplanted them into CB17-SCID/beige mice after sublethal irradiation (Tx-Rlx) (**Figure 6**). Control mice received-mock transduced bone marrow cells (Tx-Mock). This protocol resulted in engraftment rates of ~50%, *i.e.*, about 50% of bone marrow cells were positive for human CD45 at 6 weeks after transplantation.[19] Subsequent to the engraftment of transplanted HSCs, mice were injected into the mammary fat pad with BT474-M1 cells. Dox or

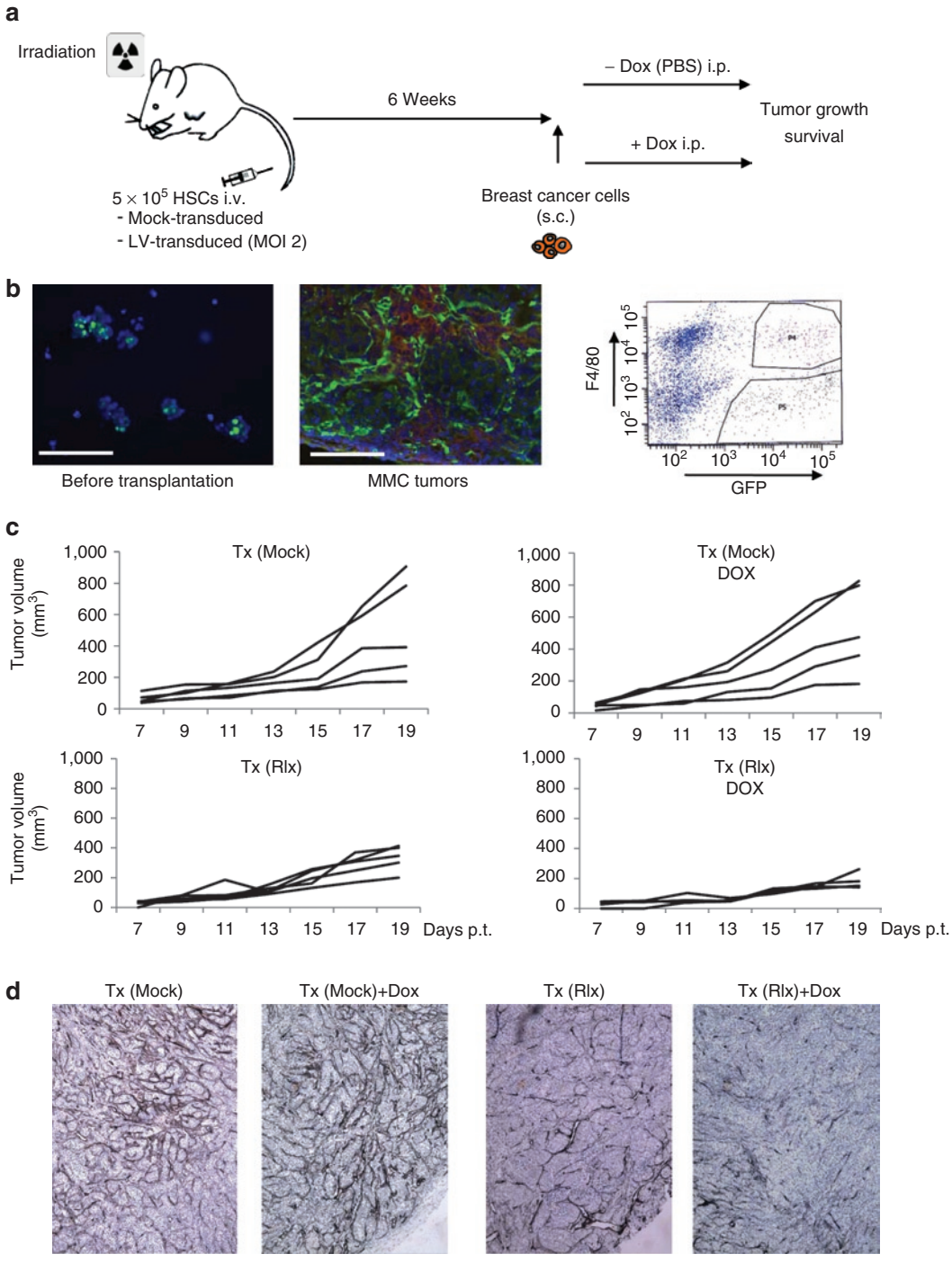

Figure 4 Studies with transplanted mouse HSCs in *neu*-tg mice carrying MMC tumors. (**a**) Scheme of experiment. A total of 5 × 10^5 of mock- or LV-transduced HSCs were transplanted into lethally irradiated *neu*-tg mice via tail vein injection. Six weeks after HSCs engraftment, MMC tumors were established via injection of 5 × 10^5 MMC cells subcutaneously. Mice received intraperitoneal injection of PBS or Dox (0.5 mg/mouse in 500 µl PBS) starting at day 7 after MMC cell transplantation and then every other day. (**b**) Tumor homing of gene modified cells. Left panel: GFP expression in HSCs before transplantation, middle panel: representative MMC tumor section from mice that received LV-GFP transduced HSCs. Right panel: F4/80 and GFP flow cytometry analyses of MMC tumors from mice that received LV-GFP transduced HSCs. Tumors were digested with collagenase to generate single cell suspensions. The gated sections P4 and P5 represent $GFP^+/F4/80^+$ and $GFP^+/F4/40^-$ cells, respectively. Shown is a representative sample. (**c**) Therapy study with mice that received mock-transduced (upper panels) and Ins-SIN-LV-Rlx-transduced (lower panels) mouse HSCs. Dox or PBS was injected intraperitoneally at day 7 after MMC cell implantation and then every other day. Rlx/Dox– versus Rlx/Dox+: $P = 0.0021$ for day 19. The P value has been calculated based data from three independent experiments with different numbers of inoculated tumor cells in each experiment. The figure shows the data from animals injected with 5 × 10^5 MMC cells. (**d**) Representative sections stained for basement membrane using Jones' periodic acid silver staining method. Basement membrane appears in dark brown/black. Dox, doxycycline; GFP, green fluorescent protein; HSC, hematopoietic stem cell; LV, lentivirus; MMC, mammary carcinoma cell; PBS, phosphate-buffered saline; Rlx, relaxin.

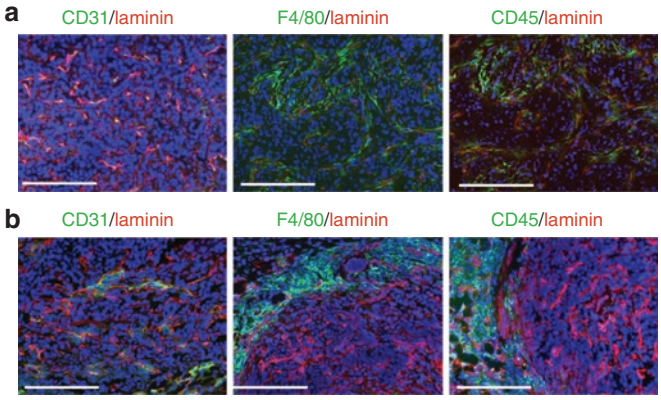

Figure 5 Infiltration of human breast cancer tumors by mouse TAMs. (**a**) BT474-M1 and (**b**) HCC1954 tumors were established in CB17-SCID-beige mice. Tumors were harvested at 4 weeks after tumor cell injection and sections analyzed for vascularization using antibodies against mouse CD31 (endothelial marker); for tumor ECM, using antibodies against mouse laminin; for leukocyte infiltration using antibodies against mouse CD45; and for TAM infiltration using antibodies against mouse F4/80. Bar = 40 µm. TAM, tumor-associated macrophage.

phosphate-buffered saline (PBS) injections started at day 7 after tumor cell transplantation and were repeated every other day. Trastuzumab treatment (10 mg/kg) was performed weekly starting at day 21 after tumor implantation. Dox treatment of mice had no effect on tumor growth (**Figure 6a**). Induction of Rlx expression in mice that were transplanted with Ins-SIN-LV-Rlx transduced HSCs markedly delayed growth of BT474-M1 tumors (**Figure 6a**); Tx (Mock)-Dox versus Tx (Rlx)-Dox: $P = 0.007$). Trastuzumab treatment of mice resulted in reduction of tumor volumes in all groups. Importantly, Dox-induced Rlx expression further increased the therapeutic effect of trastuzumab (**Figure 6b**); Tx (Mock)-trastuzumab/Dox versus Tx (Rlx) versus Tx (Rlx)-trastuzumab/Dox: $P < 0.05$. In the Tx(Rlx)/Dox/trastuzumab group, tumors disappeared in 60% of mice and did not reoccur within the monitoring period (6 weeks).

To show that the Rlx-mediated enhancement of trastuzumab therapy is mediated by ECM degradation and better access to Her2/*neu*, we analyzed tumor histology (**Figure 6c–f**). Hematoxylin and eosin staining of the tumor section from Rlx-expressing mice revealed more dispersed and smaller tumor nests compared to mice that did not express Rlx (**Figure 6c**). Her2/neu staining was comparable in all groups (**Figure 6d**). There was less staining for basement membrane and the ECM protein collagen IV in Rlx-expressing mice (**Figure 6e,f**). Quantitative image analysis of collagen IV signals revealed significantly less collagen IV in Rlx versus non-Rlx-expressing mice ($P < 0.05$). The collagen IV area per tumor section was 0.62 (+/−0.08)% in Tx(Mock) mice and 0.33 (+/−0.03)% in Tx(Rlx)+Dox mice.

As BT474-M1 tumors were sensitive to trastuzumab treatment, we tested our approach in a second model with Her2/*neu*-positive HCC1954 cells (**Figure 7**). Preliminary studies had shown that trastuzumab only marginally delayed HCC1954 tumor growth. As described above, we transplanted mice with mock-treated and Ins-SIN-LV-Rlx transduced HSCs and implanted HCC1954 tumor cells only when the transplanted cells were engrafted in the bone marrow. As in the BT474-M1 model, Dox injection had no effect on tumor growth (**Figure 7a**). Trastuzumab treatment did not significantly delay tumor growth; Tx (Mock)-PBS versus Tx (Mock)-trastuzumab: $P = 0.24$; Tx (Mock)-Dox versus Tx (Mock)-trastuzumab/Dox: $P = 0.17$). Importantly, Dox-induced Rlx expression from transplanted cells significantly delayed tumor growth; Tx (Mock)-Dox versus Tx (Rlx)-Dox: $P = 0.01$. This effect was increased by trastuzumab treatment; Tx (Rlx)-Dox versus Tx (Rlx)-Dox/trastuzumab: $P = 0.008$. Furthermore, Dox-induced Rlx expression significantly facilitated trastuzumab therapy; Tx (Mock)-trastuzumab/Dox versus Tx (Rlx)-trastuzumab/Dox: $P = 0.006$. No significant difference was found in Tx (Rlx) mice treated with PBS or Dox, although a trend toward a tumor growth delay upon Dox induction was observable. The latter result suggests that, although we used insulated vectors in this study, there was still significant Rlx background expression *in vivo* from TAMs/TAM progenitors without Dox induction. This is also reflected in Rlx mRNA levels in Tx (Rlx) mice with and without Dox treatment. Quantitative reverse transcription-PCR on total RNA isolated from tumors showed that GAPDH-normalized ΔCt values were 89.6 (+/−21.6)% for Tx (Rlx) and 156.0(+/−37.7)% for Tx (Rlx)+Dox animals higher than control values in Tx (Mock) mice. This demonstrates, significant induction of Rlx expression by Dox, but also high background Rlx expression levels without induction. To evaluate Rlx protein expression in tumors, we utilized tumor lysates for immunoprecipitation/western blot analysis with anti-Rlx antibodies. No Rlx expression was detectable in Mock-transplanted animals, whereas specific Rlx signals were present in Tx(Rlx) and Tx(Rlx)Dox animals. Quantitative analysis of Rlx-specific western blot signals showed that Rlx expression was 3.7-fold higher in Dox-treated animals (**Figure 7b**). While hematoxylin and eosin and Her2/*neu* stainings of tumor sections did not show apparent differences between groups (**Figure 7c**), collagen IV immunohistochemical analyses revealed markedly decreased collagen IV signals in tumors of Tx(Rlx)Dox compared to Tx (Mock) animals (**Figure 7d**). Based on morphometry analysis, the collagen IV area per tumor section was 6.7 (+/−1.2)% in Tx(Mock) mice, 5.3 (+/−0.7)% in Tx(Rlx), and 1.7 (+/−0.5)% in Tx(Rlx)+Dox mice ($P < 0.05$ for Tx(Mock) versus Tx(Rlx)+Dox).

In summary, we showed in two xenograft models with human Her2/*neu*-positive breast cancer cell lines that stem cell-based Rlx gene therapy delays tumor growth and allows for unfolding the therapeutic potential of trastuzumab by removing physical barriers for targeting Her2/*neu*.

DISCUSSION

This study confirms our earlier results in the *neu*/tg-MMC model that HSC-mediated Rlx expression enables control of tumor growth. As outlined above, tumor stroma is essential for tumor growth, implying that Rlx-mediated degradation of ECM should exert antitumor effects even in the absence of an active antitumor immune response, as it is the case in CB17-SCID/beige mice. We also expect that in breast cancer patients, in which, even at late stage, tumor-specific T-cells often exist, intratumoral Rlx expression as a monotherapy would exert therapeutic effects. This is based on publications demonstrating that the capability of antitumor T-cells to penetrate tumor stroma and infiltrate deep into the parenchyma correlates with an improved prognosis in breast

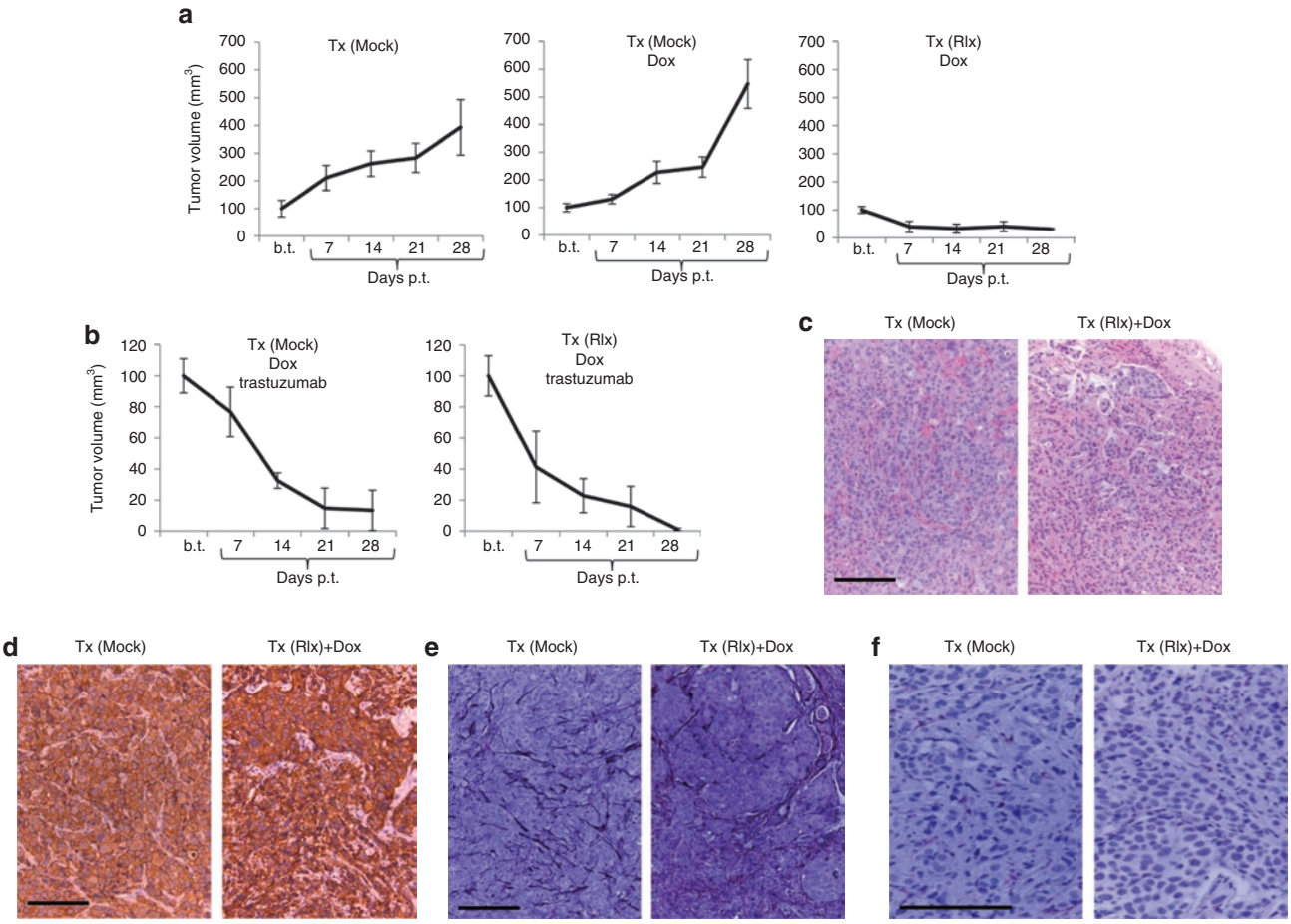

Figure 6 Therapy studies in the BT474-M1 xenograft model. CB17-SCID-beige mice were transplanted with either mock- or Ins-SIN-LV-Rlx-transduced HSCs cells [Tx (Mock) and Tx (Rlx), respectively]. After engraftment of HSCs, BT474-M1 cells were implanted into the mammary fat pad. Intraperitoneal Dox or PBS injections started 7 days after tumor cell implantation. Trastuzumab injections started 21 days after BT474-M1 cell transplantation. (**a**) Tumor growth in Tx (Mock) and Tx (Rlx) mice without trastuzumab treatment. Shown is the relative increase of tumor volume. Tumor volumes at the day on which Dox/PBS injections were started ("b.t.") were taken as 100%. b.t., before treatment; p.t., post-treatment. *N* = 7. Shown are the average tumor volumes and SD. (**b**) Tumor growth in Tx (Mock) and Tx (Rlx) mice with trastuzumab treatment. Note that the scale of the y-axis is different. (**c**,**d**) Representative tumor sections of mice without Rlx expression [Tx (Mock)] and with Dox-induced Rlx expression [Tx (Rlx)+Dox] stained with (**c**) H&E and for (**d**) Her2/*neu*. Tumors from trastuzumab-treated mice were either absent or too small and could therefore not be evaluated. (**e**,**f**) Representative sections stained for basement membrane using (**e**) Jones' periodic acid silver staining method and (**f**) collagen IV. Collagen staining in **f** appears in brown. Collagen IV stained sections were used for morphometry. Bar = 40 µm. Dox, doxycycline; GFP, green fluorescent protein; HSC, hematopoietic stem cell; LV, lentivirus; PBS, phosphate-buffered saline; Rlx, relaxin; SIN, self-inactivating.

cancer,[26] ovarian cancer,[27] lung cancer,[28] and bladder cancer[29] patients. In this context, intratumoral Rlx expression might also be able to improve various breast cancer vaccines, which, thus far, showed efficient activation of tumor-specific T and B cells,[30–35] however, lacked objective vaccine-induced cancer regression.

Our study also provides a proof-of-concept for an approach that enhances antibody-based cancer therapy in a xenograft model of Her2/*neu*-positive breast cancer as shown for trastuzumab treatment. In a model with Her2/*neu*-positive BT474-M1 tumors and the more treatment-refractory HCC1954 tumors, we observed a significant delay of tumor growth when trastuzumab therapy was combined with Dox-induced Rlx expression.

Both xenograft tumor models tested in this study adequately reflected tumor histology seen in patients *in situ*, *i.e.*, tumor stroma surrounding nests of epithelial cancer cells. For *Rlx* gene delivery, we abandoned our Ad vector-based approaches that we extensively tested in the past, as they were not efficient in tumors with this histology due to physical barriers.[1,36] We also believe that the continuous administration of recombinant human Rlx, as it has been done *e.g.*, in lung fibrosis models,[37] is clinically not feasible due to the high costs and side effects of systemic Rlx application.[38] We therefore used a "Trojan horse" stem-cell based approach. This approach is based on the fact that tumor cells secrete a number of chemokines that actively mobilize myeloid progenitors from the bone marrow and recruit them to the tumor stroma where they differentiate into TAMs. TAMs are critical for tumor survival as they produce factors that trigger/support tumor growth, neoangiogenesis, immune escape, and stroma development. Ultimately, our plan is to transduce *ex vivo*, the patient's HSCs with optimized viral vectors containing therapeutic transgenes, and transplant these stem cells into cancer patients after chemotherapy, expecting that they will engraft in the bone marrow and provide a long-term source of genetically modified cells that will home to tumors. HSC harvesting and *in vitro* transduction

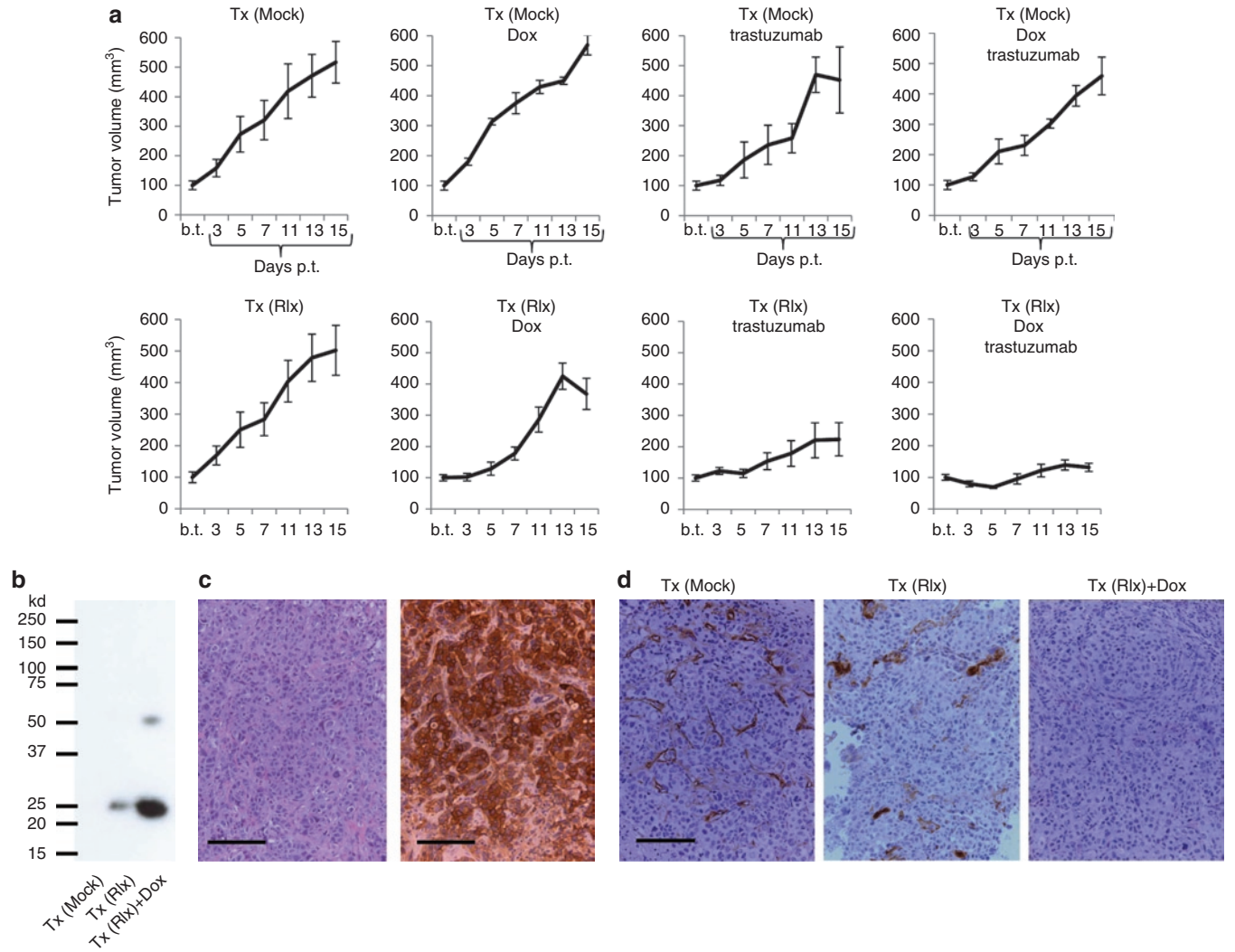

Figure 7 Therapy studies in the HCC1954 model. Mice were treated as described in **Figure 6**. (**a**) Tumor growth in mice. Shown is the relative increase of tumor volume. Tumor volumes at the day Dox/PBS injection were started ("b.t.") were taken as 100%. b.t., before treatment; p.t., post-treatment. *N* = 5. Shown are the average tumor volumes and SD. In the Tx(Rlx)Dox group, the decrease in tumor volume between days 13 and 15 is not significant. (**b**) Tumor lysates were subjected to immunoprecipitation with polyclonal anti-Rlx antibodies and analyzed by western blot with monoclonal anti-Rlx antibodies. Representative samples are shown. In agreement with the manufacturer, the monoclonal anti-Rlx antibody reacts with 25 kd and ~50 kd Rlx forms. (**c**) Representative paraffin sections of tumors from mice without Rlx expression [Tx (Mock)] stained with H&E (left panel) and for Her2/*neu* (right panel). Tumor sections for the other experimental groups were similar. (**d**) Immunohistochemistry for collagen IV. Positive signals appear in brown. Bar = 40 µm. Dox, doxycycline; GFP, green fluorescent protein; H&E, hematoxylin and eosin; HSC, hematopoietic stem cell; LV, lentivirus; PBS, phosphate-buffered saline; Rlx, relaxin; SIN, self-inactivating.

are clinically well-established procedures and the HSC transplantation can be embedded into the chemotherapy cycles that the patient receives for cancer treatment. An advantage of using HSCs over mesenchymal stem cells, which have been employed as gene delivery vehicles in cancer therapy studies,[39,40] is that after transplantation into myelo-conditioned recipients, HSCs engraft and provide a life-long source of genetically modified cells, specifically of TAMs, which represent the predominant cell type of inflammatory infiltrates of breast cancer.

Tranduction of human $CD34^+$ cells with murine leukemia virus-based retrovirus vectors has been used in clinical trials for genetic blood diseases such as SCID-ADA, SCID-X1, and sickle cell disease.[41] A critical problem with the use of murine leukemia virus-based retroviruses became apparent in X-SCID trials, where a number of patients developed leukemia due to insertional mutagenesis and activation of an oncogene(s). However, several recent studies in tumor-prone mouse models have demonstrated that tumorigenesis does not occur with SIN-lentivirus vectors and the use of insulated vectors would decrease the potential risk even more.[41] We have considered these findings in our approach and developed insulated SIN-lentivirus vectors that allowed for Dox control of Rlx expression *in vitro* in breast cancer cell lines. *In vivo* in xenograft tumors, however, we found significant *Rlx* mRNA expression without Dox induction. This indicates that chromatin insulators or Dox-inducible systems appear to function less efficiently *in vivo* in cells derived from HSCs.

As transduced HSCs not only home to tumors but also to normal organs,[19] Rlx is also expressed at extratumoral sites. In

agreement with previous studies, we did however not observe pathological changes in organ histology and hematological parameters. This might be due to the fact that Rlx inhibits collagen expression when collagen is overexpressed *i.e.*, in tumors; it does not markedly alter basal levels of collagen expression, in contrast to other collagen-modulatory cytokines, such as interferon-γ.[37] Based on recent evidence that TAMs have a unique gene expression signature that distinguishes it from other tissue macrophages,[42] we are currently working on TAM-specific expression systems in the context of insulated SIN-lentivirus vectors to increase the safety of our approach.

There are concerns that tumor stroma degradation by Rlx increases metastasis. Studies by Silvertown *et al*. reported that permanent Rlx overexpression increased *in vivo* prostate xenograft tumor growth and angiogenesis.[43] These results were recently revised by the same group.[44] The general consensus is now that Rlx expression alone is not sufficient to induce metastasis, a process that involves epithelial to mesenchymal transition, dissociation of cells from the primary tumor, enhanced cell motility, and the ability of cells to invade blood vessels.[15,45,46] Notably, in studies involving Ad-mediated Rlx expression, no metastases were found.[15,16] In fact, Ad-mediated Rlx expression reversed the spread of tumor cells that normally would metastasize.[15] Along this line, Rlx expression in this and our previous[19] studies did not result in metastasis.

Our study has also potential relevance for other experimental or established breast cancer therapies, including T-cell therapy. Adoptive T-cell therapy, *i.e.*, the infusion of tumor-competent T-cells, has, so far, not achieved significant therapeutic benefit. Among the obstacles that affect this type of therapy are physical stromal barriers produced by the host–cancer interaction, which prevents access of immune effectors to the cancer.[47,48] A detailed analysis of an infused HER-2/*neu*-specific CD8-positive T cell clone in a patient with breast cancer, suggests that tumor stromal factors may be preventing intratumoral diffusion of T cells.[49] Another application of HSC-based Rlx expression could be in combination with encapsulated chemotherapy drugs. In this context, it is notable that several liposomal formulations or albumin conjugates of platinum drugs are now used clinically[6] and newer formulations including various polymers, nanotubes, and dendrimers, are currently under intensive clinical testing.

In summary, we show that regulated Rlx expression in breast cancer tumors after stem cell-based gene delivery is safe and significantly improves trastuzumab therapy.

Our results have implications for antibody therapy of other epithelial and nonepithelial cancers as well as for other treatment approaches that are based on T-cells or chemotherapy drugs delivered as liposomes, polymers, or nanoparticles.

MATERIALS AND METHODS

Cells. MMC cells were cultured in RPMI-1640 containing 15% fetal bovine serum (Hyclone, South Logan, UT), 1% Penicillin/Streptomycin, and 1% L-glutamine (Invitrogen, Eugene, OR). HCC1954 (human breast cancer cells) were cultured in RPMI-1640 containing 10% fetal bovine serum, 1% Penicillin/Streptomycin, and L-glutamine. BT474-M1 is a tumorigenic subclone of BT474.[50] BT474-M1 cells were cultured in Dulbecco's modified Eagle's medium/F:12 with 10% fetal bovine serum, 1% Penicillin/Streptomycin, and L-glutamine.

To obtain mouse HSCs, donor mice were injected with 5-fluorouracil (150 mg/kg) intravenously 2 days before bone marrow isolation. Bone marrow cells were cultured for 3 days, and nonadherent cells were collected for lentivirus infection and transplanted on the next day into irradiated donor mice.

Antibodies. The following antibodies were used in immunohistochemical studies: rat anti-mouse CD31 (BD Pharmingen, San Jose, CA), rat anti-mouse CD45 (BD Pharmingen), rat anti-mouse F4/80 (Abcam, Cambridge, MA), goat antihuman collagen IV (Southern Technology, Longwood, FL), rabbit anti-laminin (DAKO, Glostrup, Denmark), mouse anti-Her2/*neu* (Abcam), anti-mouse Ig-AlexaFluor 488 (green) (Invitrogen, Molecular Probes, Eugene OR), anti-rabbit Ig-AlexaFluor 568 (red) (Molecular Probes).

Rlx activity assay. The activity of Rlx in culture supernatants was measured based using a cAMP bioassay as described elsewhere.[22]

Animal experiments. All experiments involving animals were conducted in accordance with the institutional guidelines set forth by the University of Washington. All mice were housed in specific pathogen-free facilities. Immunocompetent rat Her2/*neu* transgenic mice (*neu*-tg) or CB17 SCID-beige were used.

HSC/MMC model: A total of 5×10^5 lentivirus vector-transduced bone marrow cells from 5-fluorouracil-treated mice were transplanted into lethally irradiated (1,050 cGy) female *neu*-tg mice. Six weeks after bone marrow transplantation, mice received 5×10^5 MMC cells by subcutaneous injection.

Human xenograft model: Transplant recipients were 6–10-week old, female CB17 SCID-beige mice, sublethally irradiated with 350 cGy immediately before tail vein injection with 6×10^5 lentivirus vector-transduced bone marrow cells from 5-fluorouracil-treated mice. After engraftment of cells in the recipients' bone marrow was confirmed, a total of 4×10^6 BT474-M1 or HCC1954 were injected into the mammary fat pad. The tumor volume was calculated using the formula [largest diameter × (smallest diameter)^2]. Mice were sacrificed when the tumor volume reached 1,000 mm^3 or ulcerated.

Immunohistochemistry for human cancer tissue sections. Paraffin sections of breast cancer tissues were analyzed using anti-laminin and anti-collagen IV antibodies. Antigen retrieval was performed on deparaffinized sections by incubation in distilled water overnight at 60 °C. Endogenous peroxidase was blocked with 3% hydrogen peroxide in PBS for 10 minutes at room temperature (RT). To prevent nonspecific signals, an Avidin/Biotin block (Vector Labs, Burlingame, CA) was used. Sections were incubated with primary antibody (1:2,000) overnight at 4 °C before being rinsed twice with PBS. The secondary antibody [biotinylated anti-rabbit (1:300) in 1% bovine serum albumin/PBS] was incubated for 30 minutes at RT. ABC solution was used as detection system. Sections were counterstained with methyl green, dehydrated and mounted.

Immunocytochemistry for* in vitro *staining of cell cultures. Cells were cultured on chamber slides (5×10^4) until they reached 75% confluence. Cells were fixed with acetone: methanol (1:1 vol/vol) for 15 minutes at 4 °C. Primary antibodies were incubated at RT for 1 hour. Anti-Her2/*neu*, -laminin, and -collagen IV antibodies were utilized. After three washes with PBS, glass slides were mounted using VECTASHIELD with DAPI (Vector Labs). Photographs were taken with a Leica DFC300FX digital camera. Confocal images were taken on a Zeiss META confocal microscope using 40× or 100× oil lenses and Zeiss 510 software (Zeiss MicroImaging, Thornwood, NY).

Immunohistochemistry for mouse tissue and organs. Tumors were embedded in optimal cutting temperature medium and frozen at −80 °C. Sections were cut at a thickness of 8 μm and fixed in methanol: aceton (1:1 vol/vol) at −20 °C for 10 minutes. Nonspecific binding was blocked by 2% nonfat dry milk in PBS for 20 minutes at RT. Primary antibodies were

incubated at RT for 1 hour. We used anti-Her2/*neu*, -laminin, -collagen IV, -mouse CD31, -mouse CD45, -mouse F4/80 antibodies. The basement membrane of the tumors was visualized using Jones' methenamine silver staining method.[25]

Morphometry. Images of anticollagen IV labeled paraffin tumor sections were taken using a Leica DFC300FX digital camera with a Leica DMLB microscope (Leica, Wetzlar, Germany). Ten ×20-magnification pictures per tumor section (five sections per tumor, collected at a distance of 100 µm) were analyzed using the Image-Pro Plus program (Media Cybernetics, Bethesda, MD) and the collagen IV-positive area (% collagen IV area per tumor section or mm^2 collagen IV/mm^2 tumor section) was calculated.

Quantitative reverse transcription-PCR. Quantification of Rlx mRNA was performed as described elsewhere.[19] mRNA extraction was performed with RNAeasy kit (Qiagen, Valencia, CA). Complementary DNA was synthesized by reverse transcription (QuantiTect Reverse Transcription kit; Qiagen). Amplification of complementary DNA was performed with SYBR GREEN mastermix (Quantace, San Mateo, CA) as described earlier.[19]

In vitro *viability assays.* 5×10^4 BT474 cells/well were seeded in triplicate in 96-well plates and grown to confluence. Trastuzumab (15 µg/ml) was added for 30 minutes and cell viability was measured 2 hours later by WST-1 assay (Roche, San Francisco, CA).

Rlx immunoprecipitation/western blot. For immunoprecipitation, the protein/G-gel crosslinking kit (Pierce, Rockford, IL) and the rat monoclonal antibody MAB2804 (R&D Systems, Minneapolis, MN) were used. Precipitated proteins were analyzed by western blot using anti-Rlx antibody ab47546-conjugated to horse radish peroxidase (Abcam). Western blot signals were quantitated using SigmaGel software.

Statistical analyses. Statistical significance of *in vivo* data was analyzed by Kaplan–Meier survival curves and log-rank test (GraphPad Prism Version 4). Statistical significance of *in vitro* data was calculated by two-sided Student's *t*-test (Microsoft Excel). *P* values <0.05 were considered statistically significant. JMP statistical package was used to perform power analysis and determine the minimal number of animals per group. Using parameters of $\alpha = 0.05$; power = 80%; effect size = 50% (80% chance of observing a difference of 50% in tumor size at a level of significance of 0.05), we arrived at a minimal group size of five for a comparison of two groups. Therefore all experiments were at least performed once with five animals per group and, if required, repeated with additional animals until significance was achieved.

ACKNOWLEDGMENTS

The work was supported by NIH grants R01 CA080192, R01 HLA078836 (A.L.), the Pacific Ovarian Cancer Research Consortium/ Specialized Program of Research Excellence in Ovarian Cancer Grant P50 CA83636, and FHCRC grant P30 DK056465 (NU). I.B. is a recipient of a postdoctoral fellowship award from "Deutsche Krebshilfe" (108988). We thank Charles Mahan and Kelly Hudkins for help with the morphometry.

REFERENCES

1. Strauss, R, Sova, P, Liu, Y, Li, ZY, Tuve, S, Pritchard, D *et al.* (2009). Epithelial phenotype confers resistance of ovarian cancer cells to oncolytic adenoviruses. *Cancer Res* **69**: 5115–5125.
2. Jain, RK (1990). Vascular and interstitial barriers to delivery of therapeutic agents in tumors. *Cancer Metastasis Rev* **9**: 253–266.
3. Wenning, LA and Murphy, RM (1999). Coupled cellular trafficking and diffusional limitations in delivery of immunotoxins to multicell tumor spheroids. *Biotechnol Bioeng* **62**: 562–575.
4. Phan, V and Disis, ML (2008). Tumor stromal barriers to the success of adoptive T cell therapy. *Cancer Immunol Immunother* **57**: 281–283.
5. Görlach, A, Herter, P, Hentschel, H, Frosch, PJ and Acker, H (1994). Effects of nIFN β and rIFNγ on growth and morphology of two human melanoma cell lines: comparison between two- and three-dimensional culture. *Int J Cancer* **56**: 249–254.
6. Harper, BW, Krause-Heuer, AM, Grant, MP, Manohar, M, Garbutcheon-Singh, KB and Aldrich-Wright, JR (2010). Advances in platinum chemotherapeutics. *Chemistry* **16**: 7064–7077.
7. Li, ZY, Ni, S, Yang, X, Kiviat, N and Lieber, A (2004). Xenograft models for liver metastasis: Relationship between tumor morphology and adenovirus vector transduction. *Mol Ther* **9**: 650–657.
8. Netti, PA, Berk, DA, Swartz, MA, Grodzinsky, AJ and Jain, RK (2000). Role of extracellular matrix assembly in interstitial transport in solid tumors. *Cancer Res* **60**: 2497–2503.
9. Davies, Cde L, Berk, DA, Pluen, A and Jain, RK (2002). Comparison of IgG diffusion and extracellular matrix composition in rhabdomyosarcomas grown in mice versus *in vitro* as spheroids reveals the role of host stromal cells. *Br J Cancer* **86**: 1639–1644.
10. Eikenes, L, Bruland, ØS, Brekken, C and Davies, Cde L (2004). Collagenase increases the transcapillary pressure gradient and improves the uptake and distribution of monoclonal antibodies in human osteosarcoma xenografts. *Cancer Res* **64**: 4768–4773.
11. Eikenes, L, Tari, M, Tufto, I, Bruland, OS and de Lange Davies, C (2005). Hyaluronidase induces a transcapillary pressure gradient and improves the distribution and uptake of liposomal doxorubicin (Caelyx) in human osteosarcoma xenografts. *Br J Cancer* **93**: 81–88.
12. Kuriyama, N, Kuriyama, H, Julin, CM, Lamborn, K and Israel, MA (2000). Pretreatment with protease is a useful experimental strategy for enhancing adenovirus-mediated cancer gene therapy. *Hum Gene Ther* **11**: 2219–2230.
13. Sherwood, OD (2004). Relaxin's physiological roles and other diverse actions. *Endocr Rev* **25**: 205–234.
14. Brown, E, McKee, T, diTomaso, E, Pluen, A, Seed, B, Boucher, Y *et al.* (2003). Dynamic imaging of collagen and its modulation in tumors *in vivo* using second-harmonic generation. *Nat Med* **9**: 796–800.
15. Ganesh, S, Gonzalez Edick, M, Idamakanti, N, Abramova, M, Vanroey, M, Robinson, M *et al.* (2007). Relaxin-expressing, fiber chimeric oncolytic adenovirus prolongs survival of tumor-bearing mice. *Cancer Res* **67**: 4399–4407.
16. Kim, JH, Lee, YS, Kim, H, Huang, JH, Yoon, AR and Yun, CO (2006). Relaxin expression from tumor-targeting adenoviruses and its intratumoral spread, apoptosis induction, and efficacy. *J Natl Cancer Inst* **98**: 1482–1493.
17. Li, Z, Liu, Y, Tuve, S, Xun, Y, Fan, X, Min, L *et al.* (2009). Towards a stem cell gene therapy for breast cancer. *Blood* **22**: 5423–5433.
18. Pohlmann, PR, Mayer, IA and Mernaugh, R (2009). Resistance to Trastuzumab in Breast Cancer. *Clin Cancer Res* **15**: 7479–7491.
19. Li, Z, Liu, Y, Tuve, S, Xun, Y, Fan, X, Min, L *et al.* (2009). Toward a stem cell gene therapy for breast cancer. *Blood* **113**: 5423–5433.
20. Emery, DW, Yannaki, E, Tubb, J and Stamatoyannopoulos, G (2000). A chromatin insulator protects retrovirus vectors from chromosomal position effects. *Proc Natl Acad Sci USA* **97**: 9150–9155.
21. Li, CL and Emery, DW (2008). The cHS4 chromatin insulator reduces γ retroviral vector silencing by epigenetic modifications of integrated provirus. *Gene Ther* **15**: 49–53.
22. Silvertown, JD, Geddes, BJ and Summerlee, AJ (2003). Adenovirus-mediated expression of human prorelaxin promotes the invasive potential of canine mammary cancer cells. *Endocrinology* **144**: 3683–3691.
23. Bostrom, J, Yu, SF, Kan, D, Appleton, BA, Lee, CV, Billeci, K *et al.* (2009). Variants of the antibody herceptin that interact with HER2 and VEGF at the antigen binding site. *Science* **323**: 1610–1614.
24. Lu, H, Knutson, KL, Gad, E and Disis, ML (2006). The tumor antigen repertoire identified in tumor-bearing neu transgenic mice predicts human tumor antigens. *Cancer Res* **66**: 9754–9761.
25. Jones, DB (1951). Inflammation and repair of glomerulus. *Am J Pathol* **27**: 991–1009.
26. Disis, ML (2010). Immune regulation of cancer. *J Clin Oncol* **28**: 4531–4538.
27. Zhang, L, Conejo-Garcia, JR, Katsaros, D, Gimotty, PA, Massobrio, M, Regnani, G *et al.* (2003). Intratumoral T cells, recurrence, and survival in epithelial ovarian cancer. *N Engl J Med* **348**: 203–213.
28. Dieu-Nosjean, MC, Antoine, M, Danel, C, Heudes, D, Wislez, M, Poulot, V *et al.* (2008). Long-term survival for patients with non-small-cell lung cancer with intratumoral lymphoid structures. *J Clin Oncol* **26**: 4410–4417.
29. Sharma, P, Shen, Y, Wen, S, Yamada, S, Jungbluth, AA, Gnjatic, S *et al.* (2007). CD8 tumor-infiltrating lymphocytes are predictive of survival in muscle-invasive urothelial carcinoma. *Proc Natl Acad Sci USA* **104**: 3967–3972.
30. Disis, ML, Goodell, V, Schiffman, K and Knutson, KL (2004). Humoral epitope-spreading following immunization with a HER-2/neu peptide based vaccine in cancer patients. *J Clin Immunol* **24**: 571–578.
31. Disis, ML, Gooley, TA, Rinn, K, Davis, D, Piepkorn, M, Cheever, MA *et al.* (2002). Generation of T-cell immunity to the HER-2/neu protein after active immunization with HER-2/neu peptide-based vaccines. *J Clin Oncol* **20**: 2624–2632.
32. Knutson, KL, Schiffman, K and Disis, ML (2001). Immunization with a HER-2/neu helper peptide vaccine generates HER-2/neu CD8 T-cell immunity in cancer patients. *J Clin Invest* **107**: 477–484.
33. Tsang, KY, Zaremba, S, Nieroda, CA, Zhu, MZ, Hamilton, JM and Schlom, J (1995). Generation of human cytotoxic T cells specific for human carcinoembryonic antigen epitopes from patients immunized with recombinant vaccinia-CEA vaccine. *J Natl Cancer Inst* **87**: 982–990.
34. Goydos, JS, Elder, E, Whiteside, TL, Finn, OJ and Lotze, MT (1996). A phase I trial of a synthetic mucin peptide vaccine. Induction of specific immune reactivity in patients with adenocarcinoma. *J Surg Res* **63**: 298–304.
35. Gilewski, T, Adluri, S, Ragupathi, G, Zhang, S, Yao, TJ, Panageas, K *et al.* (2000). Vaccination of high-risk breast cancer patients with mucin-1 (MUC1) keyhole limpet hemocyanin conjugate plus QS-21. *Clin Cancer Res* **6**: 1693–1701.
36. Strauss, R and Lieber, A (2009). Anatomical and physical barriers to tumor targeting with oncolytic adenoviruses in vivo. *Curr Opin Mol Ther* **11**: 513–522.
37. Unemori, EN, Pickford, LB, Salles, AL, Piercy, CE, Grove, BH, Erikson, ME *et al.* (1996). Relaxin induces an extracellular matrix-degrading phenotype in human lung fibroblasts *in vitro* and inhibits lung fibrosis in a murine model in vivo. *J Clin Invest* **98**: 2739–2745.
38. Guarneri, V, Lenihan, DJ, Valero, V, Durand, JB, Broglio, K, Hess, KR *et al.* (2006). Long-term cardiac tolerability of trastuzumab in metastatic breast cancer: the M.D. Anderson Cancer Center experience. *J Clin Oncol* **24**: 4107–4115.

39. Nakamizo, A, Marini, F, Amano, T, Khan, A, Studeny, M, Gumin, J *et al.* (2005). Human bone marrow-derived mesenchymal stem cells in the treatment of gliomas. *Cancer Res* **65**: 3307–3318.
40. Studeny, M, Marini, FC, Champlin, RE, Zompetta, C, Fidler, IJ and Andreeff, M (2002). Bone marrow-derived mesenchymal stem cells as vehicles for interferon-β delivery into tumors. *Cancer Res* **62**: 3603–3608.
41. Nienhuis, AW, Dunbar, CE and Sorrentino, BP (2006). Genotoxicity of retroviral integration in hematopoietic cells. *Mol Ther* **13**: 1031–1049.
42. Stearman, RS, Dwyer-Nield, L, Grady, MC, Malkinson, AM and Geraci, MW (2008). A macrophage gene expression signature defines a field effect in the lung tumor microenvironment. *Cancer Res* **68**: 34–43.
43. Silvertown, JD, Ng, J, Sato, T, Summerlee, AJ and Medin, JA (2006). H2 relaxin overexpression increases *in vivo* prostate xenograft tumor growth and angiogenesis. *Int J Cancer* **118**: 62–73.
44. Silvertown, JD, Symes, JC, Neschadim, A, Nonaka, T, Kao, JC, Summerlee, AJ *et al.* (2007). Analog of H2 relaxin exhibits antagonistic properties and impairs prostate tumor growth. *FASEB J* **21**: 754–765.
45. Samuel, CS, Hewitson, TD, Unemori, EN and Tang, ML (2007). Drugs of the future: the hormone relaxin. *Cell Mol Life Sci* **64**: 1539–1557.
46. Turley, EA, Veiseh, M, Radisky, DC and Bissell, MJ (2008). Mechanisms of disease: epithelial-mesenchymal transition–does cellular plasticity fuel neoplastic progression? *Nat Clin Pract Oncol* **5**: 280–290.
47. Blankenstein, T (2005). The role of tumor stroma in the interaction between tumor and immune system. *Curr Opin Immunol* **17**: 180–186.
48. Singh, S, Ross, SR, Acena, M, Rowley, DA and Schreiber, H (1992). Stroma is critical for preventing or permitting immunological destruction of antigenic cancer cells. *J Exp Med* **175**: 139–146.
49. Bernhard, H, Neudorfer, J, Gebhard, K, Conrad, H, Hermann, C, Nährig, J *et al.* (2008). Adoptive transfer of autologous, HER2-specific, cytotoxic T lymphocytes for the treatment of HER2-overexpressing breast cancer. *Cancer Immunol Immunother* **57**: 271–280.
50. Lee, C, Dhillon, J, Wang, MY, Gao, Y, Hu, K, Park, E *et al.* (2008). Targeting YB-1 in HER-2 overexpressing breast cancer cells induces apoptosis via the mTOR/STAT3 pathway and suppresses tumor growth in mice. *Cancer Res* **68**: 8661–8666.
51. Szulc, J, Wiznerowicz, M, Sauvain, MO, Trono, D and Aebischer, P (2006). A versatile tool for conditional gene expression and knockdown. *Nat Methods* **3**: 109–116.
52. Aker, M, Tubb, J, Groth, AC, Bukovsky, AA, Bell, AC, Felsenfeld, G *et al.* (2007). Extended core sequences from the cHS4 insulator are necessary for protecting retroviral vectors from silencing position effects. *Hum Gene Ther* **18**: 333–343.